Supplementary Materials for

Pushing of the oocyte nucleus by growing microtubules polarises the *Drosophila* dorsal-ventral axis.

Tongtong Zhao, Owen S. Graham, Alexandre Raposo, and Daniel St Johnston

correspondence to: d.stjohnston@gurdon.cam.ac.uk

This PDF file includes:

Materials and Methods
Figs. S1 to S6

Other Supplementary Materials for this manuscript includes the following:

Movies S1 to S15

Materials and Methods

Fly stocks and genetics

The following fly stocks were used. Cam-GFP (protein trap collection (*31*)), Cam-RFP (generated from Cam-GFP by a P-element swap), *Ubi*-EB1-GFP (*32*) *Ubi*-Cnn-GFP (*33*), *Ubi*-PACT-GFP (*34*), *Ubi*-Sas4-GFP (*35*), *Ubi*-Dlic-GFP (gift of J. Raff), *UASp*-EB1-GFP (*36*), FRT82B*DSas4*^{S2214}/TM6c (*37*), *par-1*^{6323}/CyO (*23*), *par-1*^{W3}/CyO (*23*), *grk*^{2B6}/CyO (*38*), *grk*^{2E12}/CyO (*38*), D*Lis-1*^{E415}/CyO (*6*), D*Lis-1*^{13209}/CyO (*6*), *BicD*^{r5}/CyO (*39*), *Df(2L)TW119*/CyO; *P[whsBicD]-94}*/+ (*5*). *DSas4*^{S2214} mutant germline clones were generated using the hsFlp/FRT*ovo*^{D} system (*40, 41*) and heat-shocking the larvae at 37°C for 2 h on four consecutive days. The *UASp*-EB1-GFP construct was expressed with a *mat-α4tub-Gal4* driver.

Antibody staining

Fixation and staining were performed according to standard protocols (fix in 10% PFA for 8 min). The following concentrations were used: rabbit polyclonal anti-Mud, 1:500 (gift of H. Nash (*42*)); mouse monoclonal anti-Lamin Dm0 (DSHB), 1:250; mouse monoclonal anti-BicD (DSHB), 1:200.

Time-lapse imaging

Ovaries were dissected into a drop of Voltalef oil 10S (VWR International) and imaged on a combined Yokogawa CSU22 spinning disk confocal imaging system with an iXon DV855 camera (ANDOR Technology) and an Olympus IX81 inverted microscope. A 1.53x magnification tube was fitted between the spinning disk unit and the camera. 60x 1.35 NA Oil UPlanSApo and 100x 1.3 NA Oil UPlanSApo objectives were used to image nuclear migration and EB1-GFP movement, respectively. MetaMorph software was used to acquire the images.

Colcemid treatment

Egg chambers were dissected into an imaging chamber coated with Poly-L-Lysine (Thistle Scientific) containing an imaging solution (5 µg/mL insulin and 2.5% (vol/vol)

fetal calf serum in Schneider's medium (Sigma) (adapted from a previous protocol (*43*))). Colcemid was added to a final concentration of 400 µg/mL. Imaging was performed using a 60x 1.2 NA Water UPlanSAPO objective on the same microscope setup described above.

Laser ablation

Ovaries were dissected into a drop of Voltalef oil 10S (VWR International). Ablation was performed on an Olympus FluoView 1000 Inverted confocal microscope with a 60x 1.35 Oil UPlanSApo or 100x 1.40 Oil UPlanSApo objective. Centrosomes were ablated using the 405 nm laser at 100% intensity in turbo mode for 5 seconds. The recovery of nuclear shape was imaged at 2-6 frames per minute for 5 min.

Image analysis

For quantitative analysis of nuclear migration, xy coordinates of the nuclear outline were extracted using the PathWriter plug-in in Image J. EB1-GFP comets that grow towards the posterior nuclear indentation were manually tracked using the MTrackJ plug-in in Image J. Nuclear polarity plots were generated by drawing a line across the nucleus (3 pixel width) and using the Plot Profile function in Image J. Volocity was used for 3D reconstructions.

Automated detection of the indentation direction and correlation with direction of migration was performed using MatLab. In brief, the outlines of nuclei at individual time frames were traced manually. A circle was then constructed with its centre at the centroid of the nuclear outline, and the average radius of the nuclear outline was taken as the radius of the fitted circle. Starting from the minimal radial point (point on the nuclear outline with the shortest distance to the centroid, i.e. at the indentation), two points were detected on either side of the minimal point at which the nuclear outline intersects with the fitted circle. The direction of the indentation was defined as the vector perpendicular to the line connecting these two points.

Quantification of microtubules hitting the nuclear indentation

EB1-GFP time-lapse movies were acquired at 2 frames per second for 1 min. EB1-GFP tracks that moved towards the nuclear indentation for at least 4 consecutive frames (equivalent of 2 s) before hitting the posterior nuclear envelope were counted ($N_{[min]}$ = 15.3±1.6, or $N_{[s]}$ = 0.26±0.03). For each track, the time that the microtubule pushes for was determined by the number of frames in which EB1-GFP stays on the microtubule tip while contacting the indentation, giving an average of t = 2.77±0.14 s. These movies only capture one confocal section (depth d = 0.8 μm), however. The number of microtubules that hit the entire indentation area per second was calculated using the measured radius of the nuclear indentation, r = 4.3±0.2 μm, as ($N_{[s]}$ / 2 r d) * π r^2 = 2.1±0.2. These values result in the number of microtubules that are pushing the nucleus at any given time 5.9±0.7.

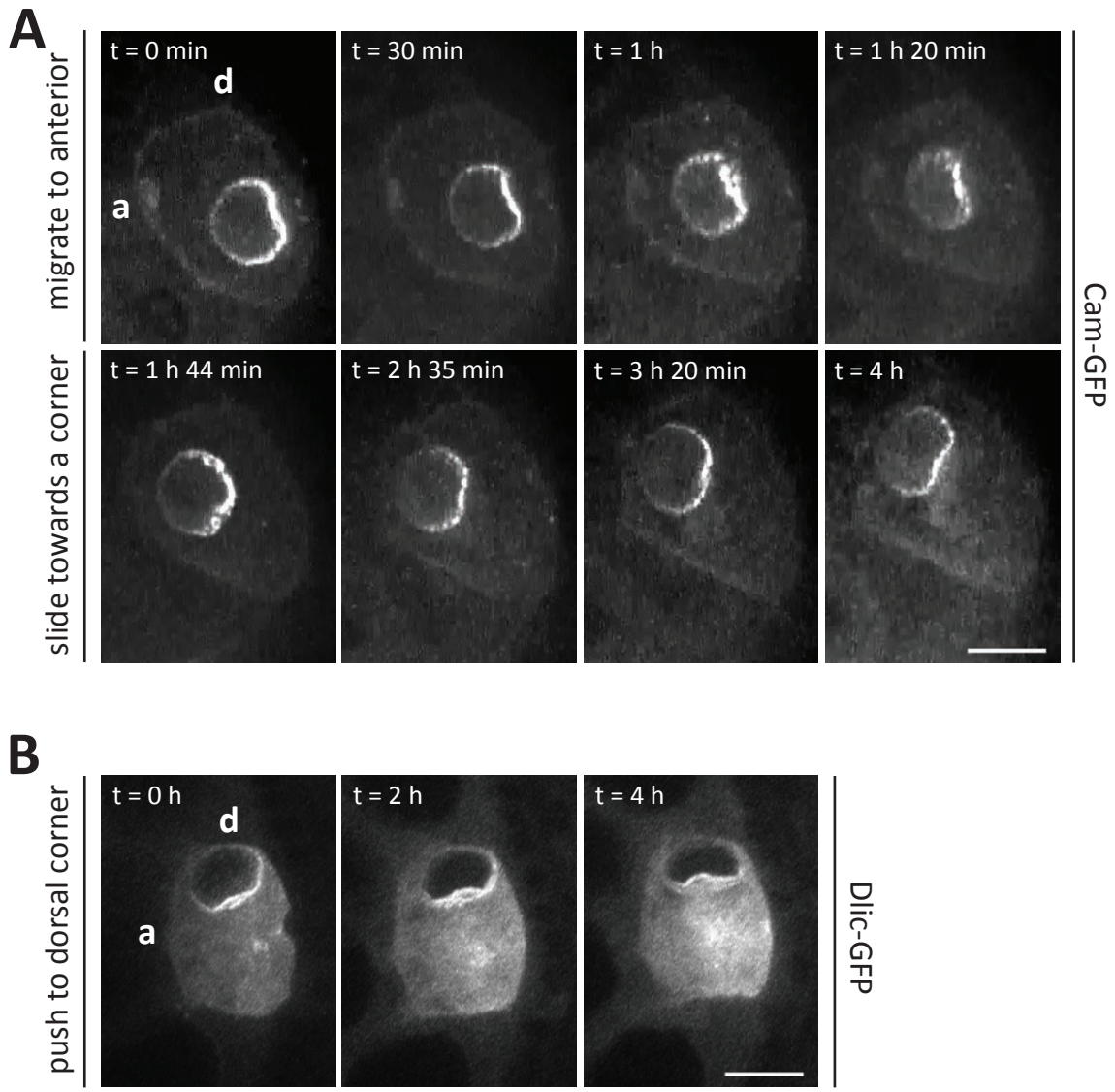

Fig. S1: Path of nuclear migration.
(**A**) In some egg chambers, the nucleus migrates towards the anterior centre, and then slides towards a random anterior corner, which will become the dorsal side. (**B**) In other cases, the nucleus appears to be already positioned at the anterior-dorsal corner at an early stage. It will then continue to be pushed into the corner. (**A-B**) a, anterior, d, dorsal; Scale bars, 10 μm.

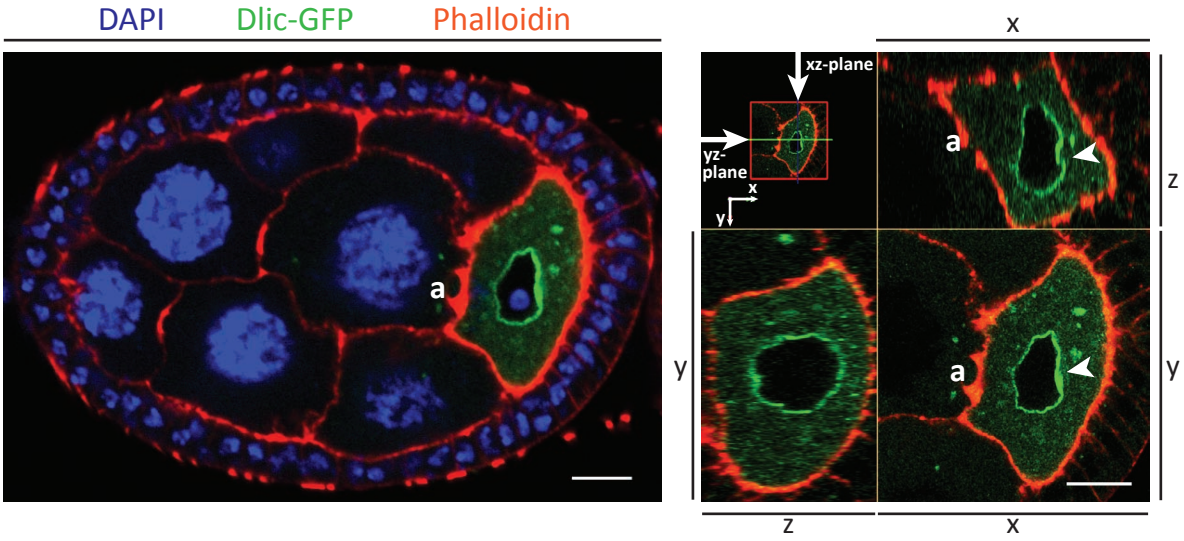

Fig. S2: Fixation confirms posterior nuclear indentation.
A stage 7 egg chamber containing a nucleus migrating to the anterior. A posterior indentation can be seen from the xy-plane and the xz-plane, but not from the yz-plane. Arrows indicate the plane of projection; arrow heads mark the indentation; a, anterior; Scale bars, 10 μm.

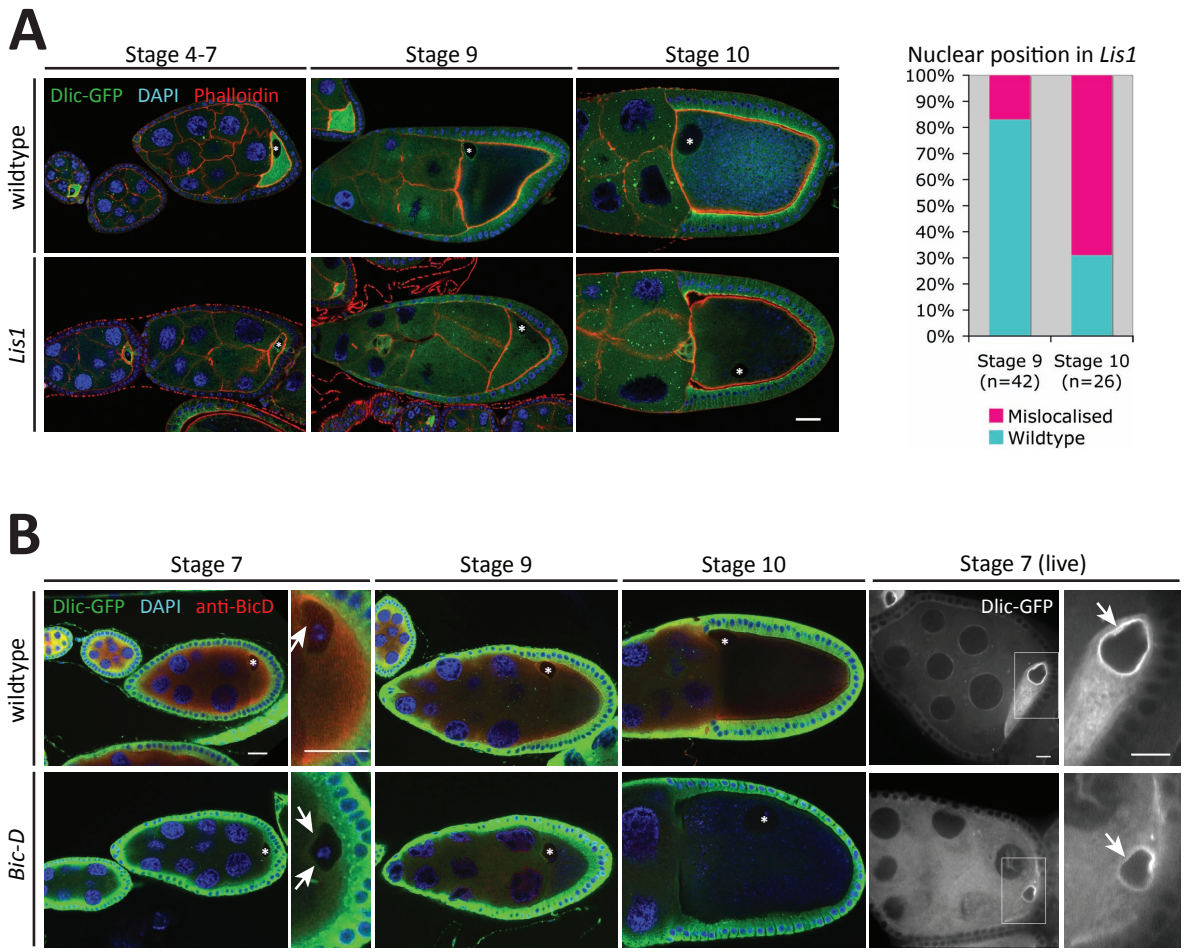

Fig. S3: Nuclear mislocalisation in mutants of dynein accessory factors is due to a failure in nuclear anchoring.

(**A**) In $Lis1^{k13209}/Lis1^{E415}$ mutants, the nucleus (asterisk) is mispositioned in stage 9 and 10 egg chambers (left-hand panels). The nuclear position at stage 7 cannot be determined due to the small size of the oocyte. Quantification shows that the proportion of mislocalised nuclei increases by a factor of four between stage 9 and 10 (right panel). Scale bar, 20 µm. (**B**) In $Bic\text{-}D^{mom}$ mutant egg chambers, the oocyte nucleus (asterisk) is correctly localised to the anterior at stage 9, but is mislocalised at stage 10. In stage 7 *Bic-D* mutant egg chambers, the oocyte is very small, and the nucleus contacts both the anterior and posterior cortex. However, both in fixed (left-hand panels) and live (right-hand panels) samples, the nucleus shows an anterior indentation (arrow), which resembles a wildtype nucleus after completion of migration, suggesting that the nucleus is anchored at the anterior. Scale bars, 20 µm (fixed) and 10 µm (live).

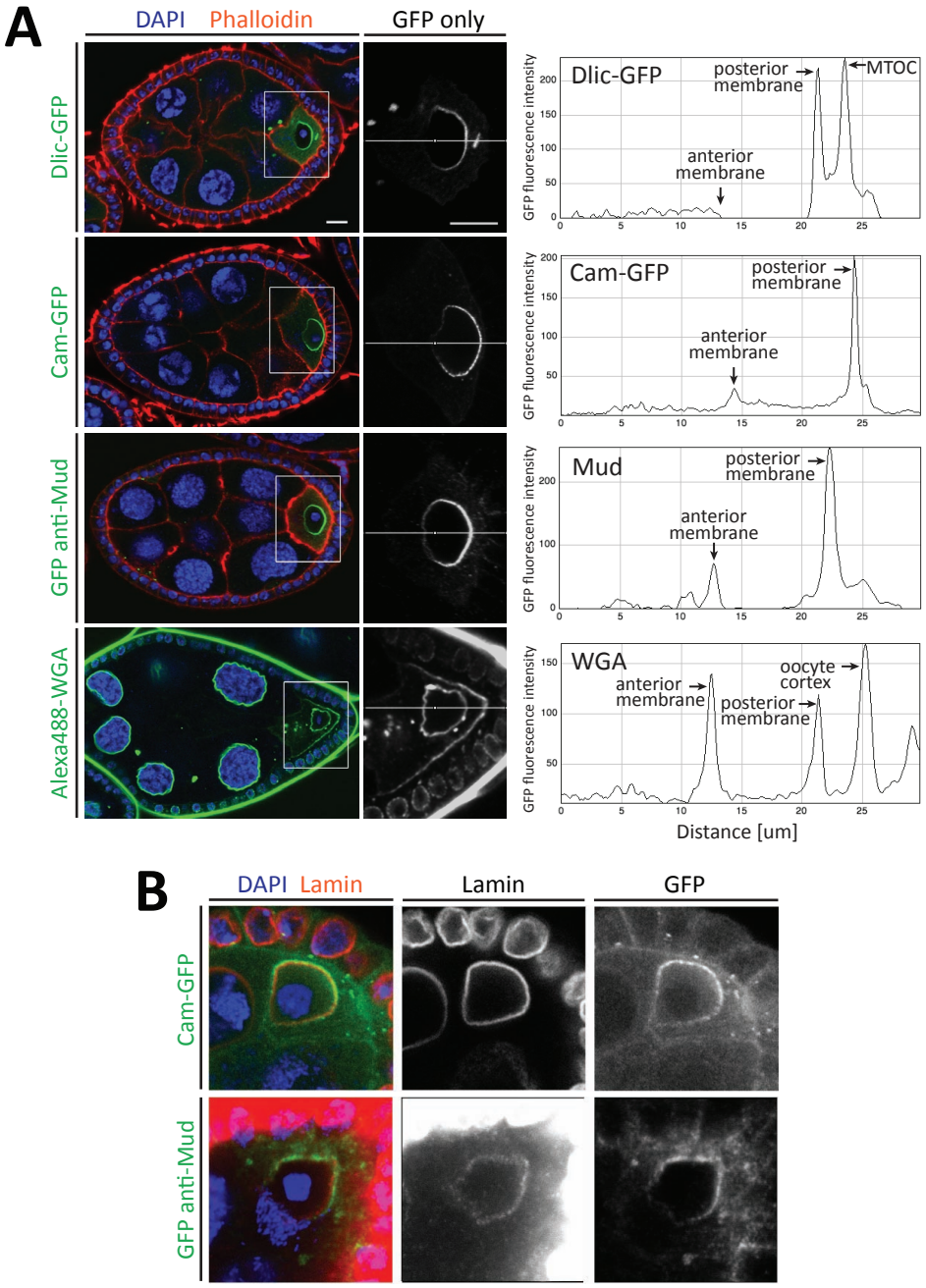

Fig. S4: Dlic-GFP, Cam-GFP and Mud are enriched on the posterior side of the nuclear membrane before and during nuclear migration.

(**A**) Confocal images of stainings (left panels) and quantification of GFP signal across the nucleus (right panels) show that Dlic-GFP, Cam-GFP, and Mud are enriched at the posterior of the nucleus. Dlic-GFP also stains the posterior MTOC. In contrast, the lectin wheat germ agglutinin (WGA) localises evenly around the nuclear membrane. Scale bars, 10 µm.

(**B**) Cam-GFP and Mud localise outside the Lamin ring, indicating that they are recruited to the outer nuclear membrane.

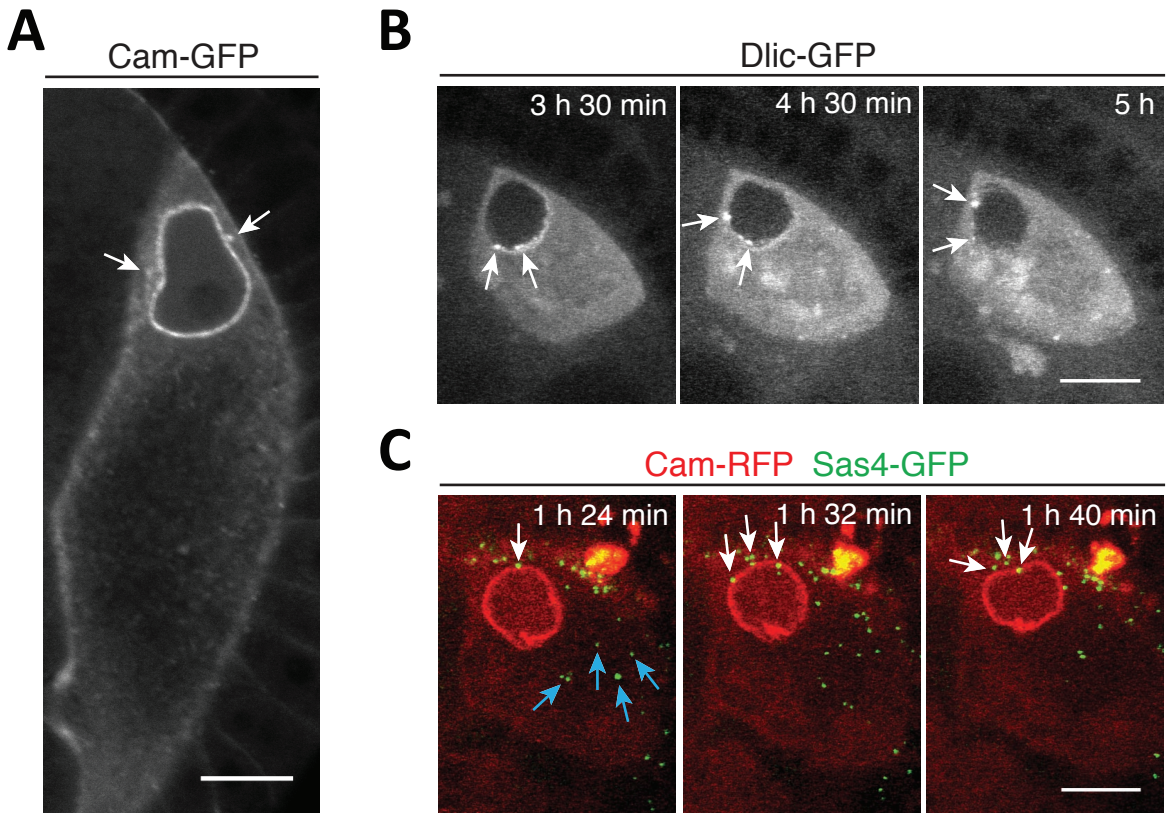

Fig. S5: Centrosome localisation at the end of nuclear migration.
(**A**) At late stage 7, centrosomes are recruited to the anterior and dorsal cortex, creating an anterior/dorsal indentation in the nucleus (arrows). (**B, C**) Centrosomes localise to the anterior-dorsal cortex either by moving along the nuclear membrane (**B**) or by recruitment from the cytoplasm (**C**). White arrows, centrosomes associated with the nucleus; Blue arrows, dispersed centrosomes in the cytoplasm. (**A-C**) Anterior is to the left, dorsal is to the top; Scale bars, 10 μm.

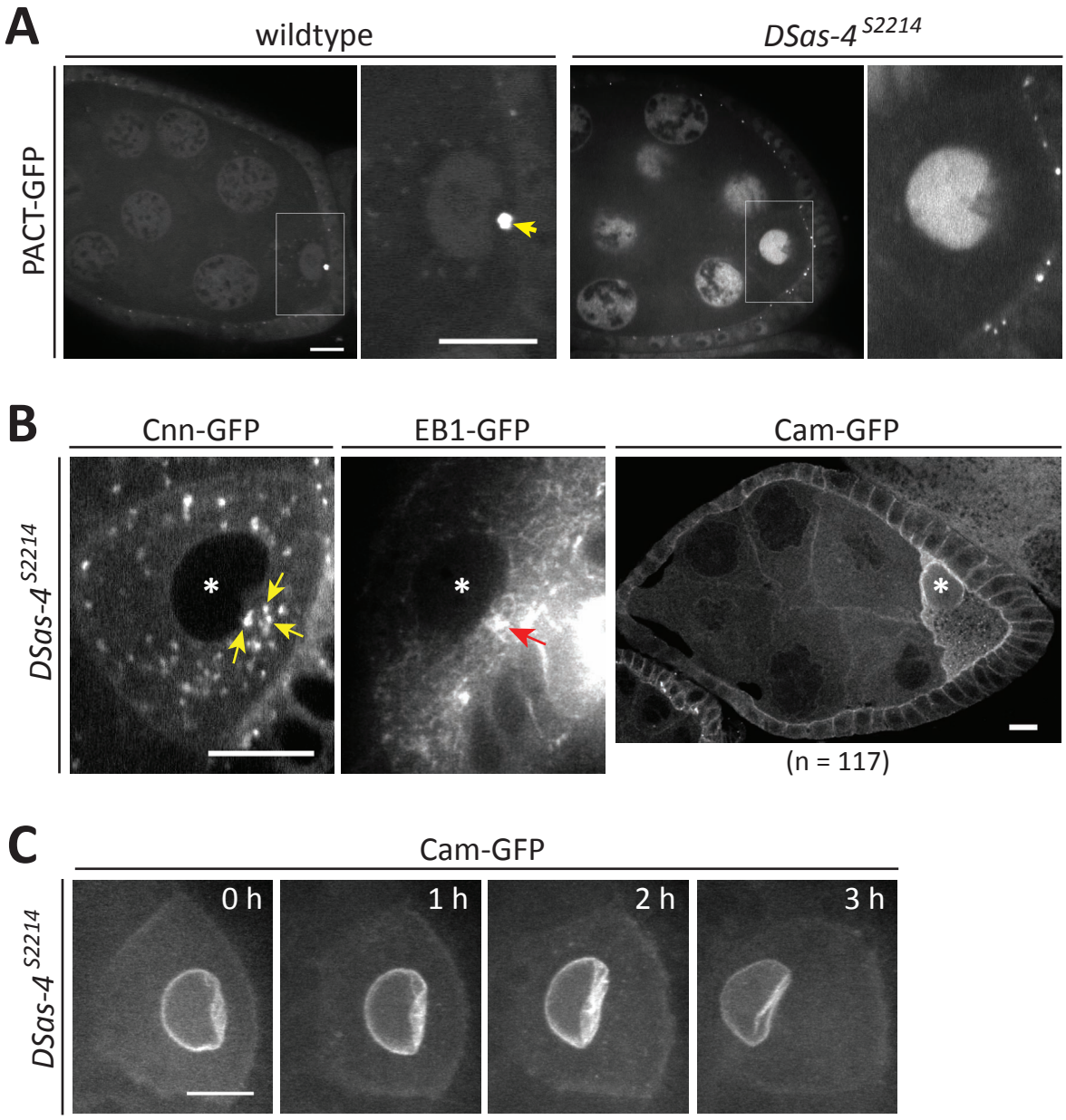

Fig. S6: The nucleus migrates normally in the absence of centrosomes.
(**A**) *DSas-4* germline clones lack centrosomes, as indicated by absence of the centriolar marker, PACT-GFP, at the posterior of the nucleus. The small puncta label the centrosomes in the somatic follicle cells, which are wildtype. (**B**) GFP-Cnn foci (arrows) still form posterior to the nucleus in *DSas-4* germline clones (left). An EB1-GFP temporal merge (20 frames, equal to 10 s) demonstrates the presence of an active MTOC behind the indentation (middle). The nucleus always migrates to the anterior dorsal cortex (right). Asterisks, oocyte nucleus. (**C**) The nucleus in *DSas-4* germline clones migrates to the anterior with a normal posterior indentation. (**A-C**) Scale bars, 10 µm.

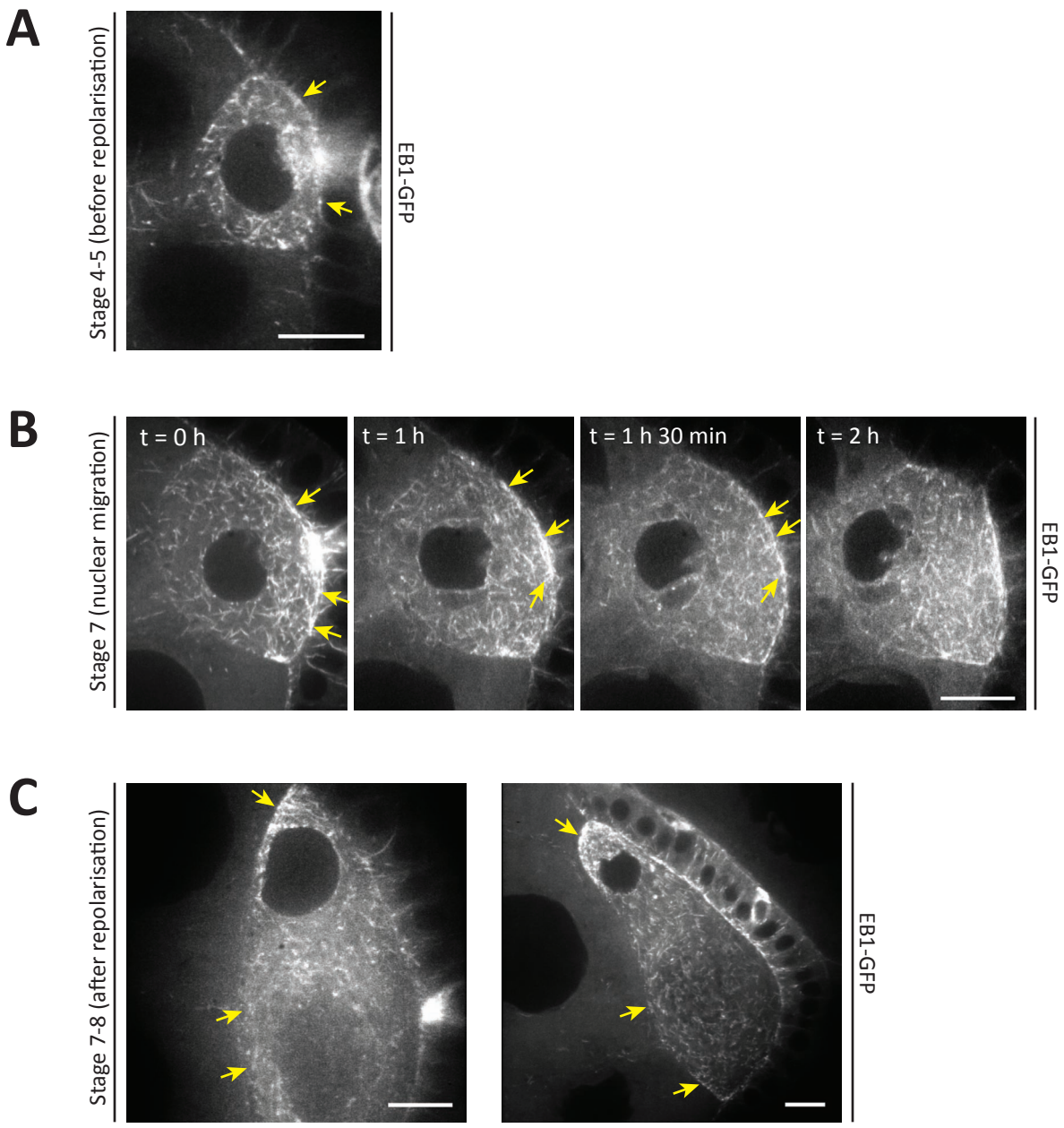

Fig. S7: Nuclear migration is independent of the microtubule array that defines the anterior-posterior axis.
(**A**) In early oogenesis, EB1-GFP is enriched in foci behind the nucleus, marking the centrosomes, and along the posterior oocyte cortex, indicating cortical microtubule nucleation sites (arrows). (**B**) An example of a nucleus that is migrating to the anterior when EB1-GFP is still enriched along the posterior oocyte cortex (arrows) and the anterior-to-posterior microtubule gradient has not yet formed. (**C**) After nuclear migration and microtubule repolarisation, EB1-GFP is cleared from the posterior cortex and is enriched along the anterior of the oocyte (arrows). 2 independent oocytes are shown.
(**A-C**) Temporal merges of 20 time frames (equal to 10 s); Scale bars, 10 µm.

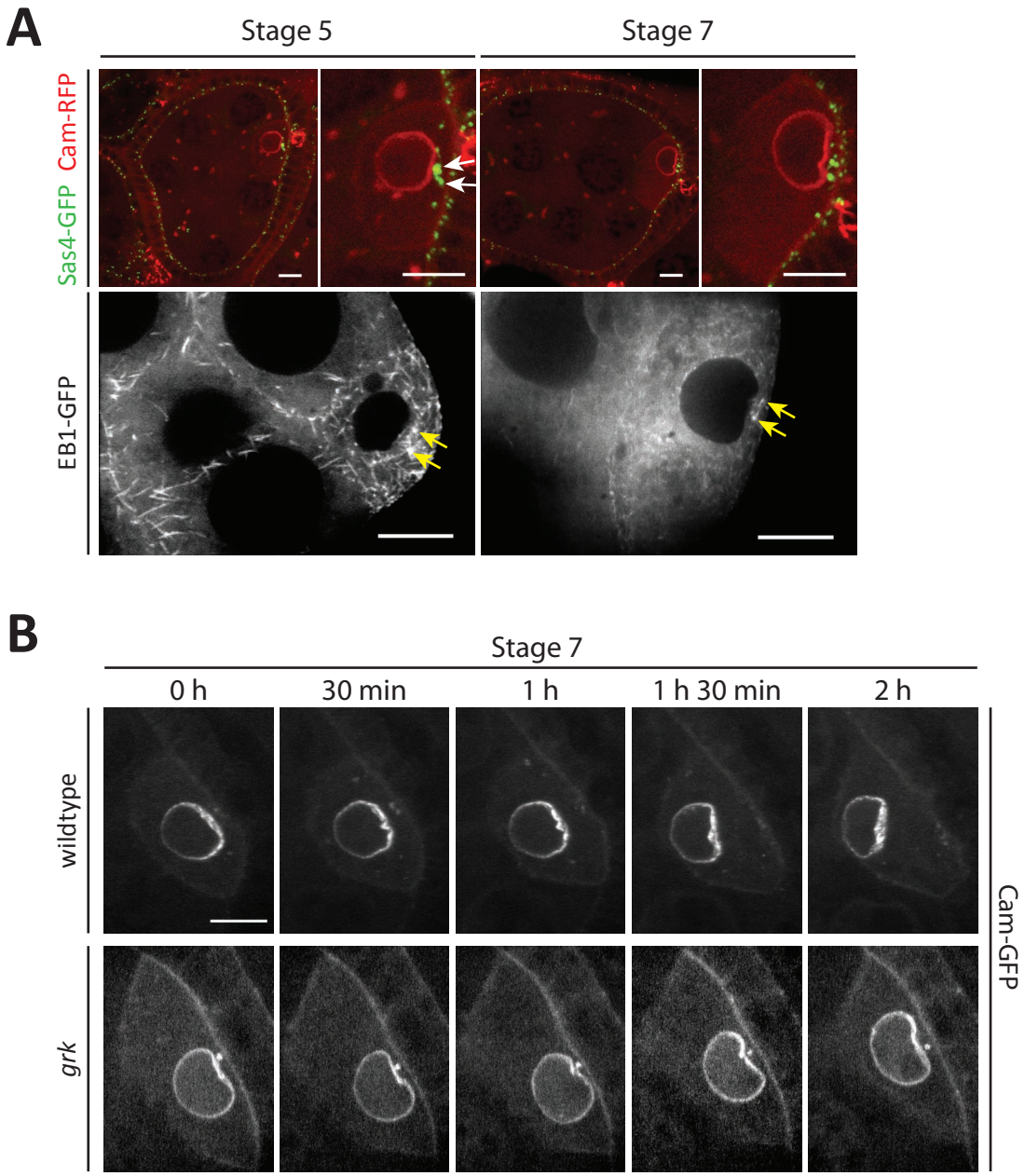

Fig. S8: The nuclear indentation is present before the onset of migration.
(**A**) A stage 5 egg chamber showing that the oocyte nucleus already has a posterior indentation. Centrosomes are localised behind the indentation. EB1-GFP temporal merges (20 frames, equal to 10 s) show an active MTOC behind the nuclear indentation in early stages. (**B**) Stills from time lapse movies showing that the nucleus has a posterior indentation in grk^{2B6}/grk^{2E12}, as in wildtype, but fails to migrate to the anterior (n=4). A slightly larger and hence older oocyte was selected for the *grk* mutant to ensure that we imaged at a stage at which the nucleus would have migrated to the anterior in wildtype. (**A-B**) Scale bars, 10 µm.